

Article

# Reduction of Stress Acting on a Thick, Deep Coal Seam by Protective-Seam Mining

Rui Gao <sup>1</sup>, Bin Yu <sup>1,2,\*</sup>, Hongchun Xia <sup>3</sup> and Hongfei Duan <sup>2</sup>

<sup>1</sup> Key Laboratory of Deep Coal Resource Mining, School of Mines, China University of Mining and Technology, Xuzhou 221116, China; cumtgaorui@163.com

<sup>2</sup> Datong Coal Mine Group Co. Ltd., Datong 037000, China; dhfcumt9@126.com

<sup>3</sup> College of Civil and Architectural Engineering, Dalian University, Dalian 116622, China; xhch@dlu.edu.cn

\* Correspondence: yubin0352@163.com; Tel.: +86-138-1346-4961

Received: 20 June 2017; Accepted: 10 August 2017; Published: 15 August 2017

**Abstract:** Aiming to reduce the high mining stress observed in large-space roof structures during mechanized mining of thick coal seams, a control technique based on protective-seam mining is proposed. This technique was used to investigate the 8108 working face of the No. 3–5 thick coal seam of the Tashan mine located in the Datong area of Shanxi, China, by means of simulations and field measurements. The numerical simulation revealed that the No. 3–5 coal seam undergoes expansion and deformation, accompanied by stress relief due to the mining of the overlying No. 4 coal seam. The physical simulation demonstrated that mining the protective seam changes the structural characteristics of the overlying strata in advance and reduces the integrity of the roof in the No. 3–5 coal seam. Field measurements showed that the support loads in the 8108 working face are significantly weaker than those in the adjacent 8107 working face, where protective-seam mining was not performed. In the absence of high resistance on the support and distinct periodic weighting characteristics, the rock masses around the 8108 working face and roadway could be easily supported.

**Keywords:** protective coal seam; thick coal seam; over-mining; stress control; strata behavior

## 1. Introduction

In China, the mining of coal seams thicker than 14 m accounts for 44% of the reserve coal resources. A sublevel-caving method is widely employed for mining because of its high efficiency and output. However, when mining thick coal seams (particularly super thick), the strata are likely to move over a wide range because the mining height is considerable, leading to complex and potentially violent strata behavior [1–6].

This is particularly so when the coal seam is covered by an overlying hard roof that breaks during mining. The long breakages, i.e., the long weighting steps, and their far-reaching effects intensify strata behaviors in the working face. Production practices [7–9] have observed frequent incidents in the supports of the working face after mining a thick coal seam with hard roof.

To control the high mining pressure occurring in the overlying structures, hydraulic fracturing and blasting has been developed to deal with the stress concentration based on weakening the hard roof [5,10–14]. Hydraulic fracturing is achieved by using fracturing equipment and high pressure water [12]; the blasting is done by placing an explosive in the borehole [14]. Through such methods, the overlying strata with well-developed fractures are more likely to cave. In this case, the stress reduction could be achieved and safety mining could be guaranteed. Moreover, Yu et al. put forward a technique of ground drilling fracturing, combined with underground pre-splitting, to control the stress concentration in coal seams and hard roofs [5]. Thus, high pressure, which is generally managed passively, can be actively pre-controlled to achieve a favorable effect. Although weakening the properties of the strata is an effective method of controlling the high mining pressure, this method is

difficult to perform and is expensive. Hence, it is necessary to develop other effective techniques to control high mining pressures.

A protective seam usually exists in the upper area of the target mining coal seam. Because mining a protective seam changes the fracture characteristics and the stress distribution of the overlying strata, mining plays an important role in releasing the pressure. Hence, outburst prevention and pressure-relaxing effects in protective coal seams have been studied in China and worldwide. For example, Wang et al. studied the technology of protective seam mining and mining sequences to aid gas control in high-gas outburst coal seam groups [15]. Dong and Zou studied a novel method for selecting seams protective against coal and gas outbursts, the results showing that the extraction of the upper protective seam caused significant decreases of stress concentration and outburst risks [16]. Liu et al. and Sun et al. focused on the challenges resulting from deep mining and put forward the technology of protective seam mining and backfill mining to realize the high stress and gas control [17,18]. However, aiming at the stress reduction and control of rock and gas outbursts, other scholars also focused on protective seam mining [19–24].

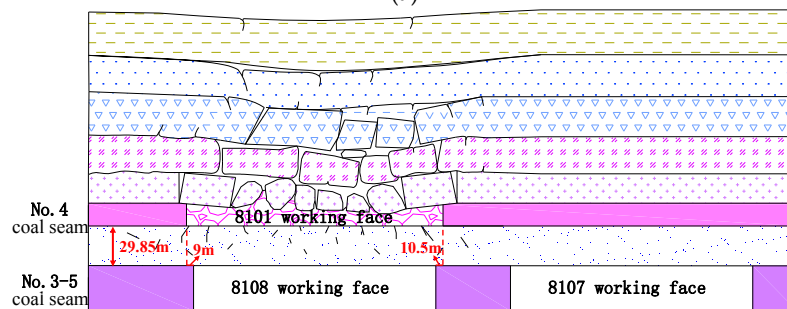
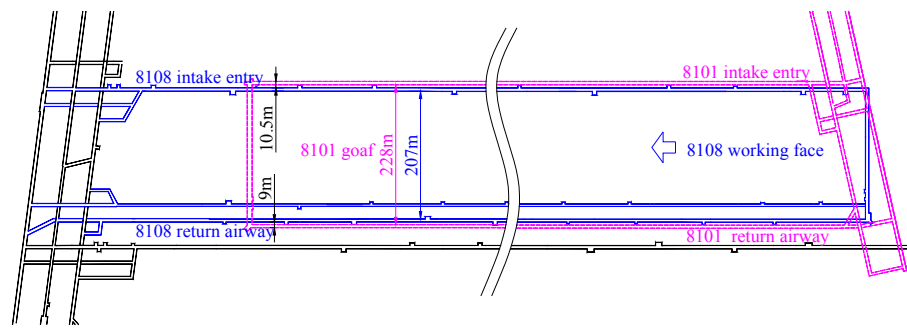
But the mining thickness of a protective coal seam and the height of the fractured overlying strata are generally small. Thus, further investigation is required to understand whether high mining pressures in large mining spaces can be controlled while mining the thick coal seams. This study was conducted on the 8108 working face of the No. 3–5 thick coal seam of the Tashan mine located in the Datong mining area in China. The Tashan No. 4 coal seam overlies the No. 3–5 coal seam. Despite the low mining thickness of the protective coal seam and the small height of the fractured overlying strata, the overlying No. 4 coal seam was first mined for research purposes. In this study, numerical and physical simulations were conducted to analyze the stress distribution of the surrounding rocks and the characteristics of the strata movement resulting from protective coal-seam mining. Subsequently, the simulations were validated through field measurements. Accordingly, the method employed is feasible and effective in controlling the high mining pressure in large mining spaces while mining the thick coal seams.

## 2. Engineering Background

In the Datong mining area, the No. 3–5 thick coal seam of the carboniferous system is predominantly mined. The seam depth and thickness of this coal seam varies in the ranges of 400–800 m and 10–20 m, respectively. The overlying strata largely comprise hard roofs, and a high mining pressure is observed in the process of mining. In the Tashan mine, the length of the 8107 working face of the No. 3–5 thick coal seam is 207 m. The mining thickness and seam depth are 14–18.42 m and 470 m, respectively. Although the working face is supported via high-resistance ZF15000/28/52 supports, support-crushing accidents frequently occur.

The length, seam depth, and thickness of the adjacent 8108 working face are 207 m, 467 m, and 16 m, respectively. For the overlying No. 4 coal seam, the length and average seam thickness of the 8101 working face are 228 m and 3.27 m, respectively. The No. 4 coal seam is at a distance of 29.85 m from the No. 3–5 coal seam.

The 8108 and 8101 working faces are internally staggered. The distance between the left and right side on the exterior of the roadway in the 8108 working face is 10.5 m. The equivalent distance for the 8101 working face is 9 m. The No. 3–5 and No. 4 coal seam were mined using the longwall-mining technique. Figure 1 shows the specifications of the layout and borehole lithology.



Columnar	Lithology	Burial Depth	Thickness	Density g/cm <sup>3</sup>	Compressive Strength/MPa	Tensile Strength/MPa	Cohesion /MPa	Friction Angle/°	Elastic Modulus/GPa	Poisson's Ratio
	Sandy mudstone	110	110	2.52	41.20	3.12	1.23	29.40	29.0	0.24
	Siltstone	212.63	102	2.67	49.67	4.90	1.96	22.52	32.15	0.23
	Quartz sandstone	227.63	15	2.53	63.00	6.20	2.01	27.06	34.25	0.22
	Sandy mudstone	297.63	70	2.52	40.20	3.03	1.20	28.70	25.67	0.24
	Siltstone	348.81	51.18	2.67	51.23	5.21	1.86	22.12	32.76	0.25
	Medium-coarse sandstone	352.23	3.42	2.62	49.21	4.76	1.79	28.23	30.67	0.22
	Middle-fine sandstone	397.47	45.24	2.53	35.67	3.40	1.43	27.60	21.00	0.26
	Silt-finstone	417.64	20.17	2.59	74.97	11.03	2.10	26.10	33.80	0.19
	No.4 coal seam	420.91	3.27	1.29	32.80	2.66	1.19	28.10	22.93	0.26
	Silt-finstone	431.59	10.68	2.67	77.70	7.90	2.94	21.42	40.50	0.18
	Lamprophyre	441.59	10.00	2.63	32.89	3.54	1.02	23.87	29.67	0.25
	Mudstone	447.15	5.56	2.31	39.80	2.98	1.08	28.40	24.90	0.24
	Lamprophyre	450.76	3.61	2.66	33.67	3.60	0.90	24.00	20.00	0.25
	No.3-5 coal seam	467.38	16.22	1.31	32.20	2.62	0.83	27.40	20.90	0.26
	Packsand	499.82	32.44	2.53	63.00	6.20	1.61	27.06	29.15	0.22
	No.8 coal seam	505.11	5.29	1.27	29.20	2.56	0.65	26.32	22.65	0.28
	Sandy mudstone	516.74	11.63	2.50	39.20	2.98	1.13	28.20	25.87	0.26
	Quartz sandstone	540.22	23.48	2.53	58.96	5.88	1.51	27.06	30.01	0.21

(c)

Figure 1. Location plans of 8108 and 8101 working faces and lithology of borehole; (a) plan view; (b) vertical section; (c) lithology of borehole.

### 3. Numerical Simulations

#### 3.1. Numerical Model

The effects of protective coal-seam mining on the lower thick coal seam and roof were analyzed using the numerical simulation FLAC<sup>3D</sup> (Itasca, Minneapolis, MN, USA) [25], along with the characteristics of the stress relief accompanying the mining process. FLAC<sup>3D</sup> is a three-dimensional explicit finite-difference program for computation of engineering mechanics, which could solve complex problems in mechanics and geomechanics. A model was designed based on the geological conditions of the 8108 working face (the dimensions in the strike and inclination directions were taken as 1000 and 600 m, respectively). The model as a whole was divided into 620,000 units. A standard hexahedral format was used with free boundaries for the upper part, as shown in Figure 2.

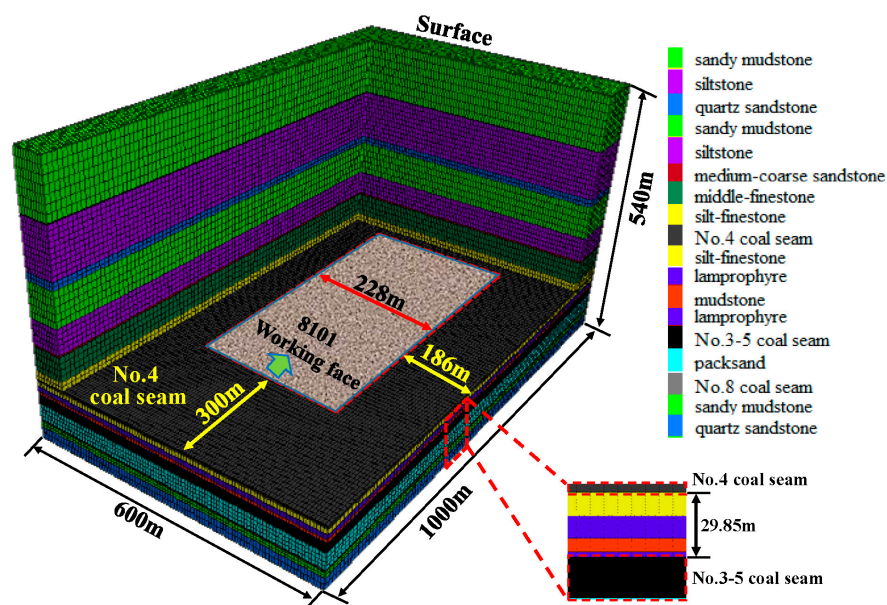


Figure 2. Numerical model.

The relevant calculations were performed in accordance with the Mohr–Coulomb yield criterion [26]. Figure 1 shows the main mechanical parameters employed in the model. The mechanical parameters of the coal seam and rock mass were obtained from laboratory experiments.

The lateral boundaries of the model were fixed in displacement at the horizontal direction, the bottom boundary was fixed in displacement at the horizontal and vertical direction, and the top boundary was set free. No loads were loaded at the top and gravitational stress was used in the model. As the lateral boundaries were fixed, the horizontal stress of the model was automatically calculated by FLAC. The advanced step of the longwall face was set as 10 m, and 40 steps were simulated. The equilibrium of each step was evaluated by the maximal unbalanced force in FLAC. To simulate the roof caving, both the coal seam and immediate roof are extracted in the process of modeling. During the extraction, the goaf area was filled by a very soft elastic material to approximately simulate the support capability of the fallen rock from the roof [26].

#### 3.2. Results

##### 3.2.1. Stress Evolution

From the simulations, the variation of the vertical stress in the No. 3–5 coal seam was obtained during the mining process of the No. 4 coal seam, as shown in Figure 3.

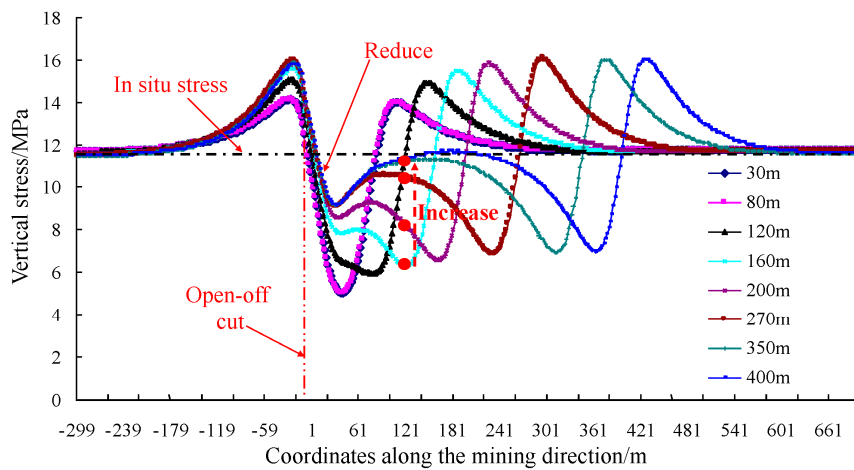
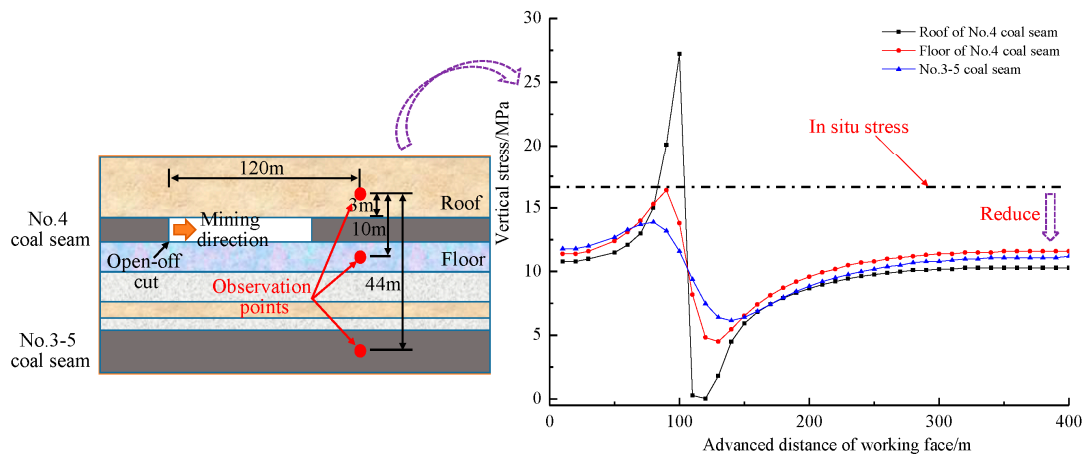


**Figure 3.** Vertical-stress curve for the No. 3–5 coal seam in the mining of the No. 4 seam.

The figure shows that because of the pressure-relieving effect of overlying No. 4 coal seam mining, the stress in the No. 3–5 coal seam was reduced in a region that located 10 m away from the open-off cut in the working face of No. 4 coal seam. Moreover, the pressure started to gradually decrease to a value below the stress in the primary rocks. As the working face advanced in the No. 4 coal seam, the pressure in a region 10–15 m ahead of the open-off cut in the No. 3–5 coal seam was significantly reduced. The lowest pressure was found to be approximately 5 MPa. With further advancement, the lowest pressure gradually increased. This is because the caved roof in the Tashan No. 4 coal seam gradually compacted the strata in the floor, thereby gradually increasing the stress in the underlying No. 3–5 coal seam.

As the region of the goaf in the No. 4 coal seam was extended, the stress in the No. 3–5 coal seam gradually increased but remained less than the stress in the primary rocks. Therefore, the stresses near the open-off cut and in the advanced position of the working face were found to be the lowest. This shows that most of the supporting stresses at these positions are due to the unexcavated coal. Therefore, the pressure in the No. 3–5 coal seam was reduced.

As the working face continued to advance, the stresses acting on the roof and floor of the Tashan No. 4 coal seam varied accordingly. To understand the characteristics of the vertical-stress distribution of the roof and floor strata, observation points were established in the roof and floor of the No. 4 seam and the No. 3–5 seams in the model. Using these points, data about the mining stress around the working face was obtained (Figure 4).



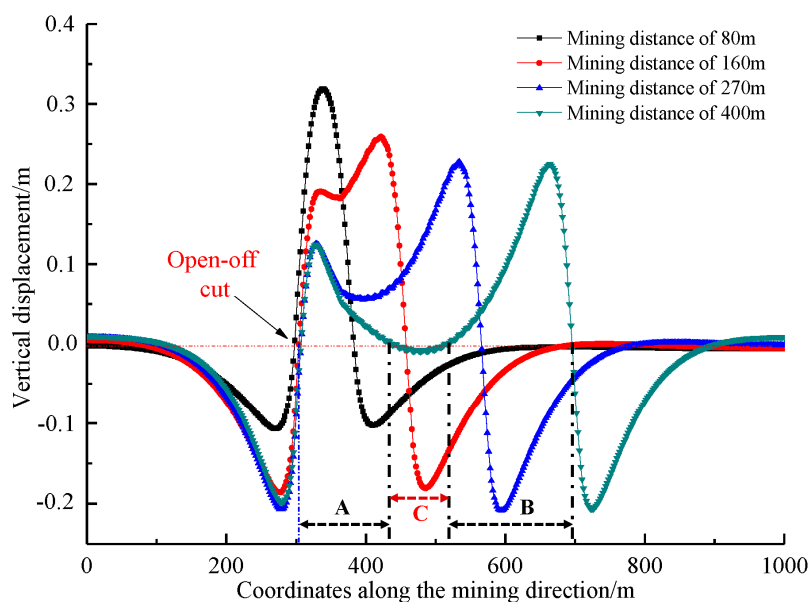
**Figure 4.** Vertical-stress distribution of different layers while mining the No. 4 coal seam.

Figure 4 shows that the stress in the roof and floor strata changed cyclically with the mining of the No. 4 coal seam. First, the stress increased, and subsequently, it decreased. Finally, the stress tended to stabilize. The figure also shows that the roof of the working face of the No. 4 coal seam was subjected to a relatively high stress, whereas a relatively low stress acted on the No. 3–5 coal seam. When the working face advanced to the observation points, the stress release was instantaneous because the roof fell on the working face. In contrast, a slight deformation and fracture (to some extent) occurred in the floor strata and the No. 3–5 coal seam. The degree of stress was observed to be the lowest in the No. 3–5 coal seam. As the working face advanced until the deformation of the overlying strata became stable, the stresses in the coal and rock strata gradually stabilized. Figure 4 shows that the supporting resistance, after the No. 3–5 coal seam stabilized, significantly reduced in comparison to the stress in the primary rocks.

As demonstrated previously, mining the protective coal seam significantly affects the surrounding rock, releasing the stresses in the rock and coal masses in advance. Moreover, the stress in the pressure-relieved areas of the floor gradually increases as the goaf becomes compacted. When the stress in the surrounding rocks varies considerably, a large number of fractures are generated.

### 3.2.2. Displacement Changes

As the No. 4 coal seam advances, the vertical displacement of the No. 3–5 coal seam is found to change (see the relevant curves in Figure 5).



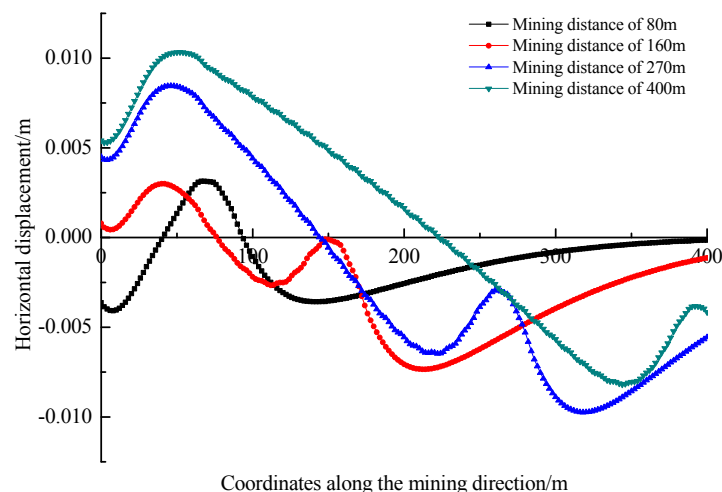
**Figure 5.** Vertical displacement of the No. 3–5 coal seam in the mining process of the No. 4 seam.

Figure 5 shows that the mining area of the protective coal seam significantly affects the protected coal seam. In the early stages, the effect of mining the No. 4 coal seam on the deformation of the No. 3–5 coal seam is negligible. As the mining of the seam continues, the No. 3–5 coal seam expands, and subsequently, becomes more clearly deformed. The displacement reaches its maximum value of 0.32 m when the working face advances a distance of 80 m. Thereafter, the maximum principal stress of the No. 3–5 coal seam was restored to some extent as the working face continued to advance. Accordingly, the expansion and deformation of the coal seam gradually decreased, finally stabilizing when the working face of the No. 4 coal seam advanced a distance of 270 m. At the same time, the deformation in the No. 3–5 coal seam was still considerable in regions where the stress in the goaf was yet to recover. Taking the curve of “mining distance of 400 m” in Figure 5 as an example. The goaf in the No. 4 coal seam ranges from 300 to 700 m, and the vertical displacement distribution

of the No. 3–5 coal seam could be divided into three regions of A, B and C. In the region A and B, the roof of the No. 4 coal seam is not entirely caved in, due to the support of the coal body in the side. Thus, it has a weak compressive resistance on the No. 3–5 coal seam, resulting in a larger displacement in regions A and B of the No. 3–5 coal seam. In the middle region C, the roof of the No. 4 coal seam has sufficiently caved and the compressive stress is recovered, which has an influence on the deformation of the No. 3–5 coal seam. The vertical displacement of No. 3–5 coal seam in region C is nearly zero.

As the working face of the No. 4 coal seam advanced, the No. 3–5 coal seam was found to be successively compressed, expanded, and subsequently, slowly compressed before finally being stabilized. Under the repetitive disturbance of the stress, fractures readily developed in the No. 3–5 coal seam. When the No. 3–5 coal seam was excavated, both the supporting load and weighting strength of the working face substantially reduced while mining the coal seam as the stresses in the coal seam, roof, and floor were released.

Figure 6 shows the variation in the horizontal deformation of the No. 3–5 coal seam due to the mining of the No. 4 coal seam. The abscissa represents the relative position of the working face, while the ordinate represents the horizontal deformation of the No. 3–5 coal seam; a positive value represents movement of the coal seam in the direction of advancement and a negative value represents movement against the direction of advancement.



**Figure 6.** Horizontal displacement of the No. 3–5 coal seam while mining the No. 4 coal seam.

Figure 6 shows that when the working face of the No. 4 coal seam advances by only a small amount, the No. 3–5 coal seam moves horizontally against the mining direction. At this stage, the No. 3–5 coal seam is subjected to compression-induced unidirectional horizontal compression. As the working face advances further, two regions of the horizontal deformation become apparent in the pressure-relieved areas of the No. 3–5 coal seam. The coal seam at a certain distance ahead of the open-off cut moves horizontally in the mining direction. However, the coal seam behind the working face moves in the opposite direction. In other words, the horizontal movement of the coal seam on both sides is dissymmetric. In this case, the coal masses in the pressure-relieved areas of the No. 3–5 coal seam are more significantly damaged because of the combined action of the horizontal stretching and compressive forces. This is highly conducive to the development of secondary fractures.

## 4. Physical Simulations

### 4.1. Physical Models

Two simulations were performed, corresponding to whether the protective coal seam was mined. The overlying strata movement and the weighting characteristics of the working faces

were subsequently analyzed. A physical model with a geometrical scale of 200:1 was designed. The dimensions of the two dimensionally similar models were 3.0 m × 0.3 m × 1.4 m (length × width × height). The different rock properties were simulated by the various proportions of sand, calcium carbonate and gypsum. In addition, mica powder was used to model the bedding layers between two strata.

The unit weight of overlying strata is about 25 kN/m<sup>3</sup>, and the average unit weight of the materials used to establish the model is 15 kN/m<sup>3</sup>. The volume–weight similarity ratio of the model was determined to be 1.667:1. By calculations, it was found that the time similarity ratio is 14.14:1, and that the stress similarity ratio is 333:1. The stress due to the overlying strata of different thicknesses could be realized by applying external loads. As the simulated height of the model is 280 m, the strata that were not laid were approximately 190 m, based on the stress similarity, a compensatory load of 0.014264 MPa was gained, and applied by pressure water bags.

The experiment was divided into two schemes: (i) The No. 3–5 coal seam was directly mined without mining the No. 4 coal seam (Scheme 1), and (ii) the No. 4 coal seam was mined first with the working face set at a distance of 0.5 m from the boundary (Scheme 2).

In scheme 2, the No. 4 was mined first; after the roof in the working face of the mined coal seam was stable, the No. 3–5 coal seam was exploited. The working face was internally staggered by a distance of 10 m from the coal seam and 0.55 m from the boundary. Figure 7 shows the mining scheme.

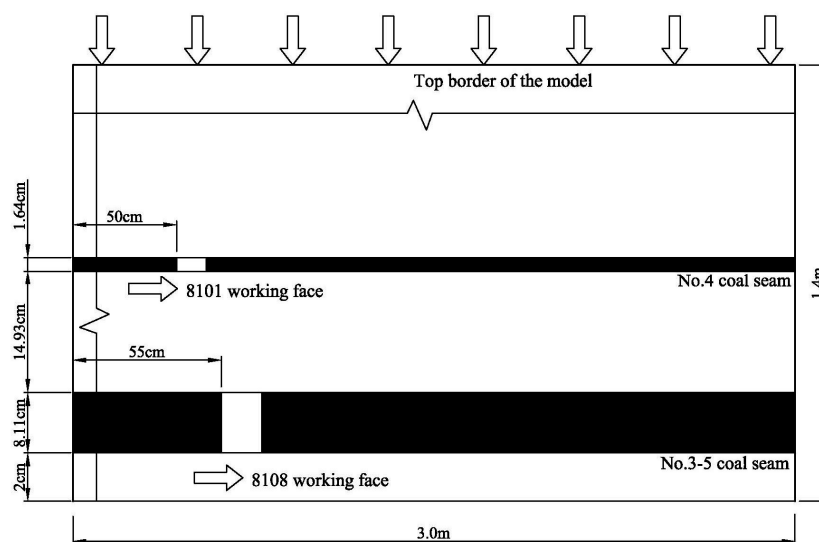


Figure 7. Experimental model scheme.

According to the mining site of the 8108 working face, there were 16 h of mining in each 24-hour period, and a mining distance of about 4 m was achieved. Based on the similarity ratio, a cycle of mining distance of 2 cm ( $4000 \text{ mm}/200 = 2 \text{ cm}$ ) every 68 min ( $16 \text{ h}/14.14 = 1.1315 \text{ h} = 68 \text{ min}$ ) was gained. The total mining distance was 1.9 m and 95 cycles were required. As for the 8101 working face of the No. 4 coal seam, there were 16 h of mining in each 24-hour period, and a mining distance of about 3.8 m was achieved. Similarly, a cycle of mining distance of 1.9 cm every 68 min was achieved. The total mining distance was 2 m and 105 cycles were required.

## 4.2. Results

### 4.2.1. Fracture Characteristics: Scheme 1

Figure 8 shows the fracture characteristics of the overlying strata while mining the No. 3–5 thick coal seam, in the case where the overlying coal seam above the working face was not excavated.

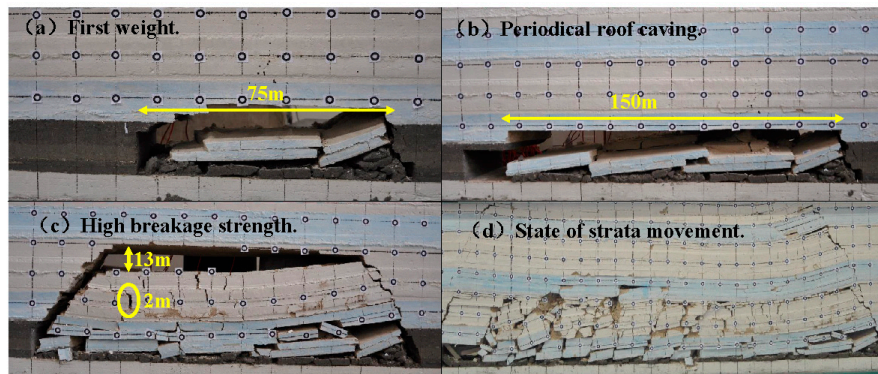


**Figure 8.** Fracture characteristics of strata without mining the No. 4 coal seam.

When the working face advanced by 77.5 m from the open-off cut, the immediate roof of the working face caved in for the first time. Because of high intensity mining and caving space in the working face, the immediate roof fell and struck the floor, thereby breaking the rocks. This process resulted in a certain level of influence, as illustrated in Figure 8a. When the working face advanced by 110 m, periodic weighting was observed for the first time. A second periodic weighting with a step of 40 m was observed when the working face advanced by 150 m. The third periodic weighting was found to occur when the working face advanced by 165 m (a step of 15 m). Under such conditions, the overlying strata in the main roof suddenly and synchronously collapsed, accompanied by an impact phenomenon. At this time, the collapsed zone was completely separated from the primary rocks, and the fracture zone was developed to a height of approximately 24 m and a width of 2 m. In addition, the height of the above free space was up to 13 m. Therefore, the collapse of the strata overlying in the free space of the separation layer significantly affected the working face, as illustrated in Figure 8c.

The weighting characteristics repeatedly occurred in the working face as the face advanced. Overall, the behavior of the strata in the working face remained violent. The average step distance of the working face was 20.2 m. Figure 8d shows the fracture characteristics of the overlying strata.

#### 4.2.2. Fracture Characteristics: Scheme 2

Based on the design of the model, the 8101 working face of the overlying the No. 4 coal seam was mined first. Figure 9 shows the caving forms of the overlying strata during this process.

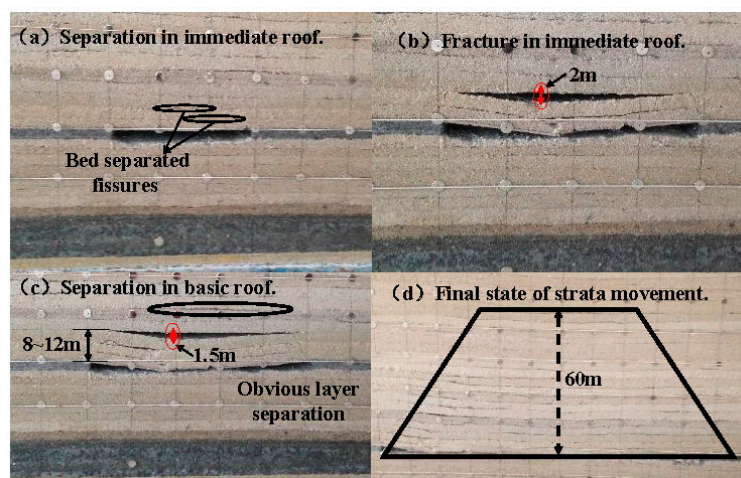


**Figure 9.** Movement characteristics of strata when mining the No. 4 coal seam.

When the working face advanced by 45 m, bed separation occurred 4 m and 8 m above the roof. As shown in Figure 9a, the bed separation increases further as the working face advances. When the working face advanced by 60 m, the immediate roof fractured for the first time at a height of 8 m. Moreover, the bed separation in the upper part was considerable, which up to a maximum distance of 2 m, as illustrated in Figure 9b.

When the working face advanced by 75 m, the immediate roof bent and periodic fractures were observed. The strata in the main roof (located 8–12 m above the coal seam) were fractured with a caving angle of  $60^\circ$ . A free motion was observed in the space above the main roof with a height of approximately 1.5 m. The above strata clearly separated, as shown in Figure 9c.

When the working face advanced to 108 m (see Figure 9d), the strata in the main roof (40 m above the coal seam) slowly subsided. At the same time, periodic fractures occurred in the underlying strata until the mining of the working face came to halt. The periodic weighting step of the working face in the No. 4 coal seam was found to be approximately 23 m, whereas the height of the fractured overlying strata was over 60 m.

Figure 10 shows the characteristics of the movement of the overlying strata while mining the No. 3–5 thick coal seam.

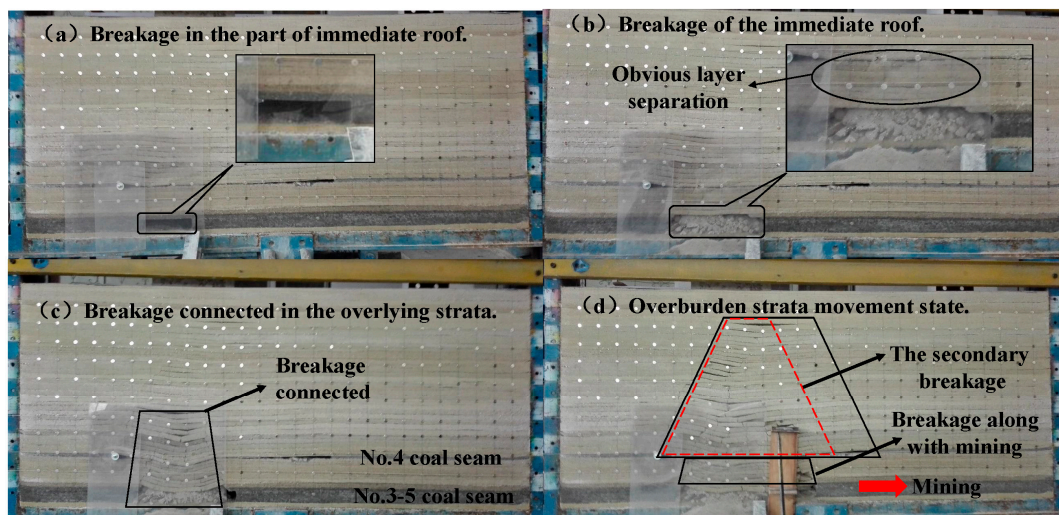


**Figure 10.** Fracture characteristics of strata while mining the No. 3–5 coal seam.

The figure shows that the fractures were generated in the overlying strata when the working face advanced by 30 m from the open-off cut. At 40 m, part of the immediate roof collapsed (Figure 10a). The immediate roof fully caved in when the working face advanced to 60 m. In addition, when the working face advanced to 70 m, the rock strata above the working face connected with the fractured strata in the No. 4 coal seam, which resulted in a certain influence. Because of the high intensity of the large mining and caving space, the overlying strata which subsided in the mining of the No. 4 seam fractured due to the mining of the No. 3–5 seam, as demonstrated in Figure 10c.

The No. 3–5 coal seam was mined up to 16.22 m, and the seam was at a distance of only 29.85 m from the No. 4 coal seam. Based on the numerical simulations, after mining the No. 4 coal seam, fractures were well-developed in the coal masses and roof of the No. 3–5 coal seam. Therefore, when the roof of the No. 3–5 coal seam connected with the overlying fractured strata of the No. 4 coal seam, it progressively collapsed with the advancement of the working face. Because of the incompleteness of the overlying strata in the protective coal seam, a secondary instability-induced failure occurred with the advancement of the working face, as shown in Figure 10d. As the intensity of the unstable secondary motion of the overlying strata significantly reduced, no clear periodic weighting characteristics were observed with the advancement of the working face in the No. 3–5 coal seam.

The fracture characteristics of the overlying strata of the working face in the No. 3–5 thick coal seam in Schemes 1 and 2 were analyzed. Table 1 presents the comparison of strata movement.

**Table 1.** Comparative analysis on the fracture characteristics of the overlying strata.

Mining Type	Characteristic of First Breakage	Periodic Roof Weighting Pace	Collapse Strength of Strata
Without liberated layer mining	77.5 m, strong impact	20.2 m	powerful
With liberated layer mining	Caving of a part of the roof when mining a distance of 40 m, and caving of the entire roof at the distance of 60 m, weak impact	No clear periodic weighting characteristics	feeble

As presented in Table 1, the mining of the protective seam shortened the first caving step of the roof while mining the No. 3–5 thick coal seam. Consequently, the periodic weighting characteristics of the working face were reduced. Thus, the magnitude of the impact of fracturing in the overlying strata reduced, thereby improving the safety and reliability of the mining of the thick coal seam.

## 5. Engineering Measurements

The 8107 working face of the Tashan mine (adjacent to the 8108 working face) is overlaid by the No. 4 integrated coal seam, which has not been mined. The working condition of the supports and the behavior of the strata in the roadways while mining the 8107 and 8108 working faces were analyzed based on the field statistics.

### 5.1. Working Resistance of the Supports

The characteristics of the supports resistance while mining the 8107 and 8108 working faces were monitored, as illustrated in Figure 11a. The results showed that the working resistance of the supports in the 8107 working face varied largely in the range of 9000–13,000 kN. The working resistances over 13,000 kN and 15,000 kN accounted for 13.96% and 6.7% of the results, respectively. Accordingly, support-crushing accidents can be frequently expected in this working face, as shown in Figure 12a. The support-crushing accidents happened three times in the 8107 working face along the mining distance of 1500 m. The first one was at the mining distance of 210 m, the crushing supports were from #35 to #75, and there were altogether 118 supports in the working face. The second crushing accident happened when the workface advanced to 400 m and the corresponding crushing supports were #31 to #82; the dynamic load factor of the supports reached 1.56. The third crushing accident was at the mining distance of 890 m; the crushing supports were #38 to #79; the dynamic load factor of the supports was 1.34.

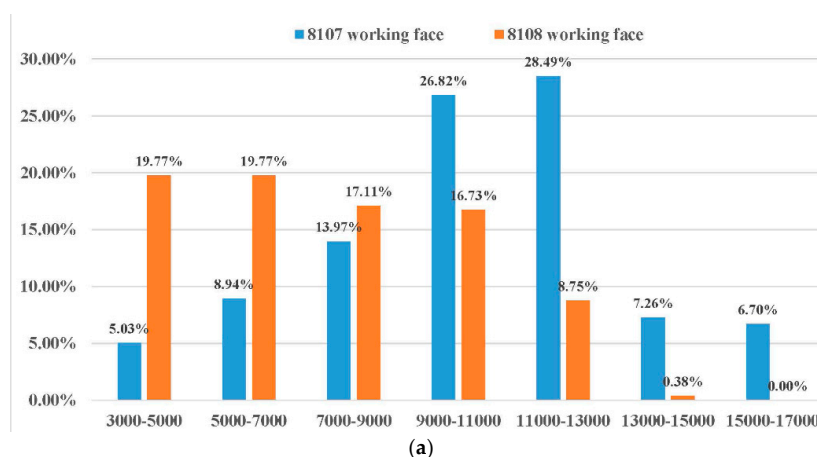


**Figure 11.** Cont.

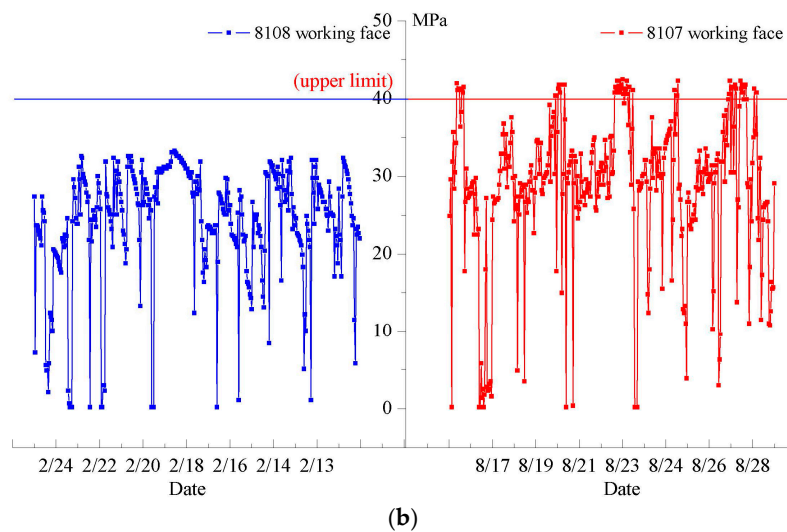


**Figure 11.** Weighing-characteristic curves for 8107 and 8108 working faces; (a) distribution of supports resistance; (b) periodic weighing characteristic.

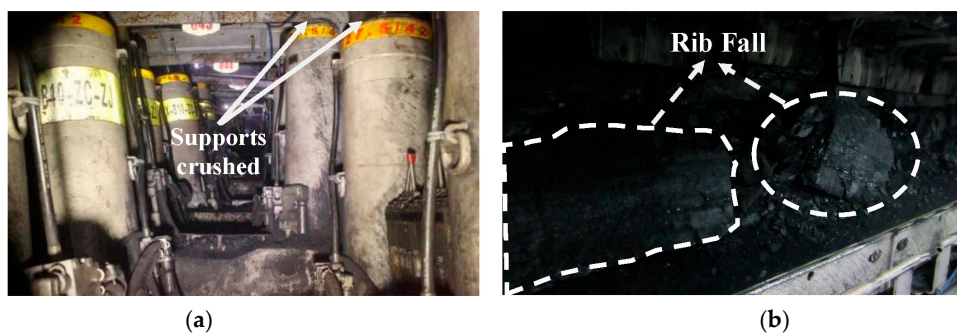


**Figure 12.** Strong strata behavior in 8107 working faces; (a) supports crushed; (b) rib fall of the coal wall.

Moreover, because of the strong strata behavior in the 8107 working face, the rib fall of the coal wall was severe and the rate of rib fall could reach 59% along the working face, as shown in Figure 12b. For the 8108 working face, the corresponding distribution is in the range of 5000–11,000 kN. The working resistances over 11,000 kN and in the range of 13,000–15,000 kN account for 9.13% and 0.38%, respectively. Accordingly, the working resistances of the supports in the 8108 working face are considerably lower than those in the 8107 working face.

The weighing characteristics observed while mining the 8108 and 8107 working faces were compared. Thus, the curves related to the working resistances of the supports could be obtained, as illustrated in Figure 11b. The figure shows that the working resistances of the supports in the 8107 working face are greater than those in the 8108 working face. According to the statistics, the working resistances of the supports in the 8107 working face occasionally exceeded their upper limit. Mining the working face by 81 m is expected to lead to five instances where the weighing exceeded the critical value (the average weighing step was 16.2 m). Thus, violent weighing events can be frequently expected in the working face. In contrast, the supports in the 8108 working face are relatively stable with no clear increase in the mining pressure. In other words, mining the 8108 working face did not lead to excessive resistance on the supports; moreover, distinct periodic weighing characteristics were absent. These observations indicate that mining the protective coal seam effectively reduces the working resistance of the supports in the working face of the thick coal seam and weakens the periodic weighing strength of the overlying strata.

## 5.2. Rock Behavior in the Roadways

The deformation of the rocks surrounding the roadways was monitored by the method of “cross measurement” while mining the 8108 and 8107 working faces. Based on the data obtained, the height of the roadway in the 8107 working face reduced from 3.6 m to 2.5 m, after moving from a distance 50 m from the advance face to a distance of 10 m. Thus, it is demonstrated that the rocks surrounding the roadway were severely deformed. The process of rock deformation in 8107 roadways is shown in Figure 13. As shown in Figure 13, when 150 m away from the working face, the deformation of the roadway is slight. As the position of the roadway is closer to the working face, the deformation of surrounding rock is more serious. Figure 13d demonstrates that when the roadway is around the working face, the roadway deformation is severe, and seriously affects safety in production. In contrast, the rocks surrounding the roadway of the 8108 working face were relatively stable. In fact, the minimum height of the deformed part of the roadway with the advancement of the working face was 3 m. Therefore, the roadway is easily supported and its integrity is favorable.

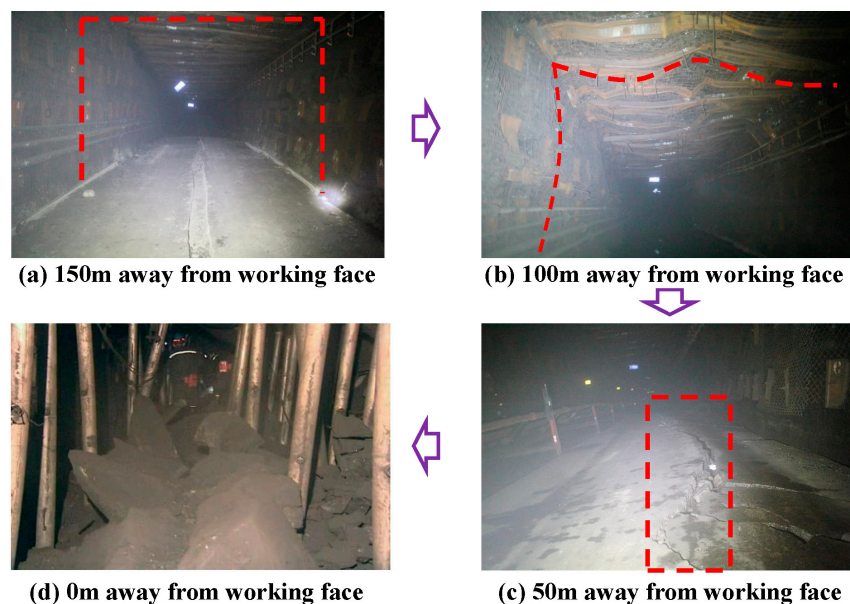


**Figure 13.** Process of rock deformation in 8107 roadways.

The above analysis shows that over-mining changes the integrity and fracture characteristics of the overlying strata in the 8108 working face. During the mining process, the roof of the working face collapsed because of the mining. Thus, a second, unstable motion occurred in the overlying strata in the protective coal seam. Moreover, the overlying strata fractured and the intensity of the unstable motion significantly reduced. Consequently, no apparent violent strata behavior was observed while mining the 8108 working face. The results suggest that protective-seam mining is an effective method of controlling adverse strata behavior while mining thick coal seams.

In the future, we will focus on developing a similar support model, and elaborating the strong strata behavior control mechanism of protective-seam mining. Meanwhile, we will fully promote the application of the technology and our analysis of its effects under different geological conditions.

The research results show that the protective-seam mining effectively reduced the strong strata behavior of thick coal seam, the deformation of the surrounding rock is controlled and the maintenance cost is saved. On the other hand, the recovery rate of coal resources is improved. Overall, the research achievement has significance in the sustainable development of energy.

## 6. Conclusions

1. The numerical analysis shows that while mining the No. 4 protective coal seam, the stable vertical stress in the No. 3–5 coal seam was lower than the stress in the primary rocks. After the No. 4 coal seam was exploited, expansion and deformation occurred in the No. 3–5 coal seam, and the maximum vertical displacement was up to 0.32 m. Under the combined action of the horizontal stretching and compression forces, fractures developed easily in the coal seam and pressure-relaxing effects were evident.
2. A similar simulation revealed that the height of the overlying strata fractured while mining the No. 4 coal seam extended up to 60 m. When the overlying coal seam was not mined in advance, the strata behavior was violent. The average weighting step of the working face was 20.2 m. No clear periodic weighting characteristics were found in the working face because of over-mining. Moreover, the effect of the roof breakage on the working faces was negligible. However, because only one single geological condition was modelled, the conclusions make weak predictions for other situations, and more models will be tested in the future.
3. In comparison to the 8107 working face, the working resistance of the supports in the 8108 working face was remarkably reduced. In the absence of clear periodic weighting characteristics in the supports, the 8108 working face could be easily supported in the roadway. Thus, protective-seam mining helps in effectively controlling the intensity of the strata behavior while mining thick coal seams.

**Acknowledgments:** This paper was supported by the Special Funding Projects of “Sanjin Scholars” Supporting Plan [NO. 2050205], and the National Key Research Projects [NO. 2016YFC0600701], and Ordinary University Graduate Student Scientific Research Innovation Projects of Jiangsu Province [NO.KYLX16\_0564].

**Author Contributions:** Rui Gao and Bin Yu conceived and designed the numerical and physical simulations; Hongchun Xia and Hongfei Duan contributed in conducting the engineering measurements; Rui Gao and Bin Yu wrote the paper.

**Conflicts of Interest:** The authors declare no conflict of interest.

## References

1. Unver, B.; Yasitli, N.E. Modelling of strata movement with a special reference to caving mechanism in thick seam coal mining. *Int. J. Coal Geol.* **2006**, *66*, 227–252. [[CrossRef](#)]
2. Alehossein, H.; Poulsen, B.A. Stress analysis of longwall top coal caving. *Int. J. Rock Mech. Min. Sci.* **2010**, *47*, 30–41. [[CrossRef](#)]
3. Li, H.M.; Jiang, D.J.; Li, D.Y. Analysis of ground pressure and roof movement in fully-mechanized top coal caving with large mining height in ultra-thick seam. *J. China Coal Soc.* **2014**, *39*, 1956–1960. (In Chinese)
4. Yu, B.; Zhao, J.; Kuang, T.J.; Meng, X.B. In situ investigations into overburden failures of a super-thick coal seam for longwall top coal caving. *Int. J. Rock Mech. Min. Sci.* **2015**, *78*, 155–162. [[CrossRef](#)]
5. Yu, B.; Zhu, W.B.; Gao, R.; Liu, J.R. Strata structure and its effect mechanism of large space stope for fully-mechanized sublevel caving mining of extremely thick coal seam. *J. China Coal Soc.* **2016**, *41*, 571–580. (In Chinese)
6. Yavuz, H. An estimation method for cover pressure re-establishment distance and pressure distribution in the goaf of longwall coal mines. *Int. J. Rock Mech. Min. Sci.* **2004**, *41*, 193–205. [[CrossRef](#)]
7. Bai, Q.S.; Tu, S.H.; Wang, F.T.; Zhang, C. Field and numerical investigations of gateroad system failure induced by hard roofs in a longwall top coal caving face. *Int. J. Coal Geol.* **2017**, *173*, 176–199. [[CrossRef](#)]
8. Tan, Y.L.; Zhao, T.B.; Xiao, Y.X. Quantitative prop support estimation and remote monitor early warning for hard roof weighting at the Muchengjian Mine in China. *Can. Geotech. J.* **2010**, *47*, 947–954. [[CrossRef](#)]
9. Zheng, Z.T.; Xu, Y.; Li, D.S.; Dong, J.H. Numerical Analysis and Experimental Study of Hard Roofs in Fully Mechanized Mining Faces under Sleeve Fracturing. *Minerals* **2015**, *5*, 758–777. [[CrossRef](#)]
10. Ge, Z.L.; Deng, K.; Lu, Y.Y.; Cheng, L.; Zuo, S.J.; Tian, X.D. A novel method for borehole blockage removal and experimental study on a hydraulic self-propelled nozzle in underground coal mines. *Energies* **2016**, *9*, 698. [[CrossRef](#)]

11. Huang, B.X.; Wang, Y.Z.; Cao, S.G. Cavability control by hydraulic fracturing for top coal caving in hard thick coal seams. *Int. J. Rock Mech. Min. Sci.* **2015**, *74*, 45–57. [[CrossRef](#)]
12. Huang, B.X.; Wang, Y.Z. Roof weakening of hydraulic fracturing for control of hanging roof in the face end of high gassy coal longwall mining: A case study. *Arch. Min. Sci.* **2016**, *61*, 601–615. [[CrossRef](#)]
13. Lu, Y.Y.; Cheng, Y.G.; Ge, Z.L.; Cheng, L.; Zuo, S.J.; Zhong, J.Y. Determination of Fracture Initiation Locations during Cross-Measure Drilling for Hydraulic Fracturing of Coal Seams. *Energies* **2016**, *9*, 358. [[CrossRef](#)]
14. Zhu, G.A.; Dou, L.M.; Li, Z.L.; Cai, W.; Kong, Y.; Li, J. Mining-induced stress changes and rock burst control in a variable-thickness coal seam. *Arab. J. Geosci.* **2016**, *9*, 365. [[CrossRef](#)]
15. Wang, H.F.; Cheng, Y.P.; Yuan, L. Gas outburst disasters and the mining technology of key protective seam in coal seam group in the Huainan coalfield. *Nat. Hazards* **2013**, *67*, 763–782. [[CrossRef](#)]
16. Dong, G.W.; Zou, Y.H. A Novel Method for Selecting Protective Seam against Coal and Gas Outburst: A Case Study of Wangjiazhai Coal Mine in China. *Sustainability* **2017**, *9*, 1015.
17. Liu, T.; Lin, B.Q.; Yang, W.; Liu, T.; Zhai, C. An integrated technology for gas control and green mining in deep mines based on ultra-thin seam mining. *Environ. Earth Sci.* **2017**, *76*, 243. [[CrossRef](#)]
18. Sun, Q.; Zhang, J.X.; Zhang, Q.; Yin, W.; Germain, D. A protective seam with nearly whole rock mining technology for controlling coal and gas outburst hazards: A case study. *Nat. Hazards* **2016**, *84*, 1–14. [[CrossRef](#)]
19. Wang, L.F.; Jiang, F.X.; Yu, Z.X. Similar material simulation experiment on destressing effects of the deep thick coal seam with high burst liability after mining upper and lower protective seams. *J. Geotech. Eng.* **2009**, *31*, 442–446. (In Chinese)
20. Li, D.Q. Mining thin sub-layer as self-protective coal seam to reduce the danger of coal and gas outburst. *Nat. Hazards* **2014**, *71*, 41–52. [[CrossRef](#)]
21. Li, W.; Cheng, Y.P.; Guo, P.K.; An, F.H.; Chen, M.Y. The evolution of permeability and gas composition during remote protective longwall mining and stress-relief gas drainage: A case study of the underground Haishiwan Coal Mine. *Geosci. J.* **2014**, *18*, 427–437. [[CrossRef](#)]
22. Jiang, J.Y.; Cheng, Y.P.; Zhang, P.; Jin, K.; Cui, J.; Du, H. CBM drainage engineering challenges and the technology of mining protective coal seam in the Dalong Mine, Tiefsa Basin, China. *J. Nat. Gas. Sci. Eng.* **2015**, *24*, 412–424. [[CrossRef](#)]
23. Liu, H.B.; Cheng, Y.P. The elimination of coal and gas outburst disasters by long distance lower protective seam mining combined with stress-relief gas extraction in the Huaibei coal mine area. *J. Nat. Gas. Sci. Eng.* **2015**, *27*, 346–353. [[CrossRef](#)]
24. Yao, B.H.; Ma, Q.Q.; Wei, J.P.; Ma, J.H.; Cai, D.L. Effect of protective coal seam mining and gas extraction on gas transport in a coal seam. *Int. J. Min. Sci. Technol.* **2016**, *26*, 637–643. [[CrossRef](#)]
25. *Fast Lagrangian Analysis of Continua in 3 Dimension*, version 3.1; Itasca: Minneapolis, MN, USA, 2007.
26. Ma, D.; Bai, H.B.; Wang, Y.M. Mechanical behavior of a coal seam penetrated by a karst collapse pillar: Mining-induced groundwater inrush risk. *Nat. Hazards* **2015**, *75*, 2137–2151. [[CrossRef](#)]

